

Global Attitude Estimation using Single Direction Measurements

Taeyoung Lee^{*†}, Melvin Leok^{*}, N. Harris McClamroch[†], and Amit Sanyal

Abstract—A deterministic attitude estimator for a rigid body under an attitude dependent potential is studied. This estimator requires only a single direction measurement to a known reference point at each measurement instant. The measurement cannot completely determine the attitude, but an attitude estimation scheme based on this measurement is developed; a feasible set compatible with the measurement is described and it is combined with an attitude dynamics model to obtain an attitude estimate. The attitude is globally represented by a rotation matrix, and the uncertainties are described by ellipsoidal sets. A numerical example for a spacecraft in a circular orbit is presented.

I. INTRODUCTION

The attitude of a rigid body is defined by the orientation of a body-fixed frame with respect to a reference frame, and the attitude is represented by a rotation matrix that is a 3×3 orthogonal matrix with determinant of 1, which transforms a representation of a vector in a body-fixed frame into one represented in the reference frame. Rotation matrices have a group structure denoted by $SO(3)$. In spacecraft applications, the attitude is usually determined by using a set of direction measurements. The directions to objects such as the sun, stars, and geomagnetic fields, assumed to be known in the reference frame, are measured in the body-fixed frame in order to determine the rotation matrix.

Attitude determination using multiple direction measurements with least squares estimation is known as Wahba's problem [1]. The original solution of Wahba's problem is given in [2], and solutions are expressed in terms of quaternions [3], and in terms of a rotation matrix [4]. Based on these attitude determination schemes, attitude estimation problems are studied in [5], [6] and [7]. The attitude determination/estimation procedures using Wahba's problem formulation require at least two different direction measurements at each measurement instant. This places a stringent constraint on the dynamic estimation of spacecraft attitude.

A single direction measurement provides some information about the attitude; it is guaranteed that the rotation

matrix lies in a one dimensional subgroup of the three dimensional special orthogonal group $SO(3)$, which is diffeomorphic to the one-sphere \mathbb{S}^1 . The attitude is not completely determined at a single measurement instant. If the process is coupled with an attitude dynamics model, an attitude estimation scheme can be developed using single direction measurements. An attitude determination scheme using single direction measurements is studied in [8], but this approach requires an additional arc length measurement.

Most existing attitude estimation schemes use generalized coordinate representations of the attitude. As is well known, minimal coordinate representations of the rotation group, such as Euler angles, lead to singularities. Non-minimal coordinate representations, like the quaternions, have their own associated problems. Besides the extra constraint of unit norm that one needs to impose on the quaternion, the quaternion representation, which is diffeomorphic to $SU(2)$, double covers $SO(3)$. So, it has an inevitable ambiguity in expressing the attitude.

A stochastic state estimator requires probabilistic models for the state uncertainty and the noise. However, statistical properties of the uncertainty and the noise are often not available. An alternative deterministic approach is to specify bounds on the uncertainty and the measurement noise without an assumption on their distribution. Noise bounds are available in many cases, and deterministic estimation is robust to the noise distribution [9]. An efficient but flexible way to describe the bounds is using ellipsoidal sets, referred to as uncertainty ellipsoids. The deterministic estimation process is based on set theory results developed in [10]; optimal deterministic estimation problems using the uncertainty ellipsoids are studied in [11] and [12].

In this paper, a deterministic attitude estimator which requires a single direction measurement at each measurement instant is presented. A feasible set in $SO(3)$ that is compatible with the measurement is represented by Lie algebra elements and the exponential map. It is compared with the attitude dynamics model to obtain an updated estimate. The estimation scheme presented in this paper has the following distinctive features: the estimator requires only a single direction measurement at each measurement instant, the attitude is represented by a rotation matrix without any local parameterization, and the deterministic estimator is distinguished from a Kalman or extended Kalman filter.

This paper is organized as follows. The attitude dynamics and uncertainty model are given in Section II. The attitude determination scheme and the attitude estimation scheme using single direction measurements are presented in Section III and IV, which is followed by a numerical example in

Taeyoung Lee, Aerospace Engineering, University of Michigan, Ann Arbor, MI 48109 tylee@umich.edu

Melvin Leok, Mathematics, Purdue University, West Lafayette, IN 47907 mleok@math.purdue.edu

N. Harris McClamroch, Aerospace Engineering, University of Michigan, Ann Arbor, MI 48109 nhm@umich.edu

Amit Sanyal, Mechanical and Aerospace Engineering, Arizona State University, Tempe, AZ 85287 sanyal@asu.edu

^{*}This research has been supported in part by NSF under grant DMS-0504747, and by a grant from the Rackham Graduate School, University of Michigan.

[†]This research has been supported in part by NSF under grant ECS-0244977.

Section V.

II. ATTITUDE DYNAMICS AND UNCERTAINTY MODEL

A. Equations of motion

We consider estimation of the attitude dynamics of a rigid body in the presence of an attitude dependent potential, $U(\cdot) : \text{SO}(3) \mapsto \mathbb{R}$, $R \in \text{SO}(3)$. Systems that can be so modeled include a free rigid body, spacecraft on a circular orbit with gravity gradient effects [13], or a 3D pendulum [14]. The continuous equations of motion are

$$J\dot{\Omega} + \Omega \times J\Omega = M, \quad (1)$$

$$\dot{R} = RS(\Omega), \quad (2)$$

where $J \in \mathbb{R}^{3 \times 3}$ is the moment of inertia matrix of the rigid body, $\Omega \in \mathbb{R}^3$ is the angular velocity of the body expressed in the body-fixed frame, and $S(\cdot) : \mathbb{R}^3 \mapsto \mathfrak{so}(3)$ is a skew mapping defined by $S(x)y = x \times y$ for all $x, y \in \mathbb{R}^3$. The vector $M \in \mathbb{R}^3$ is the moment due to the potential, determined by $S(M) = \frac{\partial U^T}{\partial R} R - R^T \frac{\partial U}{\partial R}$, or more explicitly,

$$M = r_1 \times v_{r_1} + r_2 \times v_{r_2} + r_3 \times v_{r_3}, \quad (3)$$

where $r_i, v_{r_i} \in \mathbb{R}^{1 \times 3}$ are the i th row vectors of R and $\frac{\partial U}{\partial R}$, respectively.

General numerical integration methods like the popular Runge-Kutta schemes, typically preserve neither first integrals nor the characteristics of the configuration space, $\text{SO}(3)$. In particular, the orthogonal structure of the rotation matrices is not preserved numerically. It is often proposed to parameterize (2) by Euler angles or quaternions instead of integrating (2) directly. However, Euler angles yield only local representations of the attitude and they have singularities. Unit quaternions do not exhibit singularities, but they have the manifold structure of the three-sphere \mathbb{S}^3 , and double cover $\text{SO}(3)$. Consequently, the unit quaternion representing the attitude is inevitably ambiguous. In addition, general numerical integration methods do not preserve the unit length constraint. Therefore, quaternions have the same numerical drift problem as rotation matrices.

Lie group variational integrators preserve the group structure without the use of local charts, reprojection, or constraints, they are symplectic and momentum preserving, and they exhibit good energy behavior for an exponentially long time period. The following Lie group variational integrator for the attitude dynamics of a rigid body is presented in [14]:

$$hS(J\Omega_k + \frac{h}{2}M_k) = F_k J_d - J_d F_k^T, \quad (4)$$

$$R_{k+1} = R_k F_k, \quad (5)$$

$$J\Omega_{k+1} = F_k^T J\Omega_k + \frac{h}{2}F_k^T M_k + \frac{h}{2}M_{k+1}, \quad (6)$$

where $J_d \in \mathbb{R}^{3 \times 3}$ is a nonstandard moment of inertia matrix defined by $J_d = \frac{1}{2}\text{tr}[J]I_{3 \times 3} - J$, and $F_k \in \text{SO}(3)$ is the relative attitude between integration steps. The constant $h \in \mathbb{R}$ is the integration step size, and the subscript k denotes the k th integration step. This integrator yields a map $(R_k, \Omega_k) \mapsto (R_{k+1}, \Omega_{k+1})$ by solving (4) to obtain $F_k \in$

$\text{SO}(3)$ and substituting it into (5) and (6) to obtain R_{k+1} and Ω_{k+1} . The only implicit part is (4). The actual computation of F_k is done in the Lie algebra $\mathfrak{so}(3)$ of dimension 3, and the rotation matrices are updated by multiplication. So this approach is distinguished from integration of the kinematics equation (2), and there is no excessive computational burden. We use these discrete equations of motion to propagate the attitude dynamics between measurements during the estimation process.

B. Uncertainty Ellipsoid

We describe uncertainties of the attitude dynamics by using ellipsoidal sets referred to as uncertainty ellipsoids. An uncertainty ellipsoid in \mathbb{R}^n is defined as

$$\mathcal{E}_{\mathbb{R}^n}(\hat{x}, P) = \left\{ x \in \mathbb{R}^n \mid (x - \hat{x})^T P^{-1} (x - \hat{x}) \leq 1 \right\}, \quad (7)$$

where $\hat{x} \in \mathbb{R}^n$, and $P \in \mathbb{R}^{n \times n}$ is a symmetric positive definite matrix. We call \hat{x} the center of the uncertainty ellipsoid, and P is the uncertainty matrix that determines the size and the shape of the uncertainty ellipsoid. The size of an uncertainty ellipsoid is measured by $\text{tr}[P]$ which is the sum of the squares of the semi principal axes of the ellipsoid.

The attitude dynamics evolves on the 6 dimensional tangent bundle, $\text{TSO}(3)$. We identify $\text{TSO}(3)$ with $\text{SO}(3) \times \mathfrak{so}(3)$ by left trivialization, and we identify $\mathfrak{so}(3)$ with \mathbb{R}^3 by the isomorphism $S(\cdot)$. The uncertainty ellipsoid centered at $(\hat{R}, \hat{\Omega}) \in \text{TSO}(3)$ is induced from an uncertainty ellipsoid in \mathbb{R}^6 ;

$$\mathcal{E}(\hat{R}, \hat{\Omega}, P) = \left\{ R \in \text{SO}(3), \Omega \in \mathbb{R}^3 \mid \begin{bmatrix} \zeta \\ \delta\Omega \end{bmatrix} \in \mathcal{E}_{\mathbb{R}^6}(0_6, P) \right\}, \quad (8)$$

where $S(\zeta) = \text{logm}(\hat{R}^T R) \in \mathfrak{so}(3)$, $\delta\Omega = \Omega - \hat{\Omega} \in \mathbb{R}^3$, and $P \in \mathbb{R}^{6 \times 6}$ is a symmetric positive definite matrix. An element $(R, \Omega) \in \mathcal{E}(\hat{R}, \hat{\Omega}, P)$ can be written as

$$R = \hat{R} \exp S(\zeta), \quad \Omega = \hat{\Omega} + \delta\Omega,$$

for some $x = [\zeta; \delta\Omega] \in \mathbb{R}^6$ satisfying $x^T P^{-1} x \leq 1$.

We assume that the initial conditions are bounded by a prescribed uncertainty ellipsoid

$$(R_0, \Omega_0) \in \mathcal{E}(\hat{R}_0, \hat{\Omega}_0, P_0), \quad (9)$$

where $P_0 \in \mathbb{R}^{6 \times 6}$ is a symmetric positive definite matrix that defines the shape and the size of the uncertainty ellipsoid.

III. ATTITUDE DETERMINATION WITH A SINGLE DIRECTION MEASUREMENT

In the attitude determination problem, we measure directions to points in the reference frame. We assume that the directions to these points are known in the reference frame. This either requires that the points are located far away from the spacecraft or the relative location of the spacecraft is known exactly. The directional sensor is fixed in the body-fixed frame, and the measurements are representations of the direction vectors in the body-fixed frame. The representations in the body-fixed frame are transformed into those in the reference frame by multiplication with the rotation matrix that defines the attitude of the rigid body.

A. Exact measurement

Let the direction to a known point in the reference frame be $e \in \mathbb{S}^2$, and let the corresponding vector represented in the body-fixed frame be $b \in \mathbb{S}^2$. We first assume that the direction measurement has no error, so the direction b is exact. Since we only measure a direction to a point, we normalize e and b so that they have unit lengths. The vectors e and b are different representations of the same vector from the spacecraft to the known point, and they are related by a rotation matrix $R \in \text{SO}(3)$ that defines the attitude of the rigid body

$$e = Rb. \quad (10)$$

This equation provides a two-dimensional constraint on the three-dimensional rotation matrix. Consequently, a single direction measurement does not completely determine the attitude. This corresponds to the fact that if we rotate the rigid body about the direction e in the reference frame, then the measured direction b is not changed. The rotation matrix has one-dimensional uncertainty represented by any rotation about the direction e in the reference frame, or equivalently, any rotation about the direction b in the body-fixed frame.

Suppose that $R^\circ \in \text{SO}(3)$ is a particular rotation matrix satisfying (10). This rotation matrix can be represented in several ways. For example, if b and e are not co-linear,

$$R^\circ = \exp \left[\cos^{-1}(b^T e) S \left(\frac{b \times e}{\|b \times e\|} \right) \right] \exp S(\theta^\circ b), \quad (11)$$

where the constant $\theta^\circ \in \mathbb{S}^1$ can be arbitrarily chosen. The rotation matrix that represents the attitude of the rigid body can be written in terms of R° as

$$R = R^\circ \exp [\theta S(b)] \quad (12)$$

for a $\theta \in \mathbb{S}^1$.

In summary, if the single direction to a known point is measured exactly, the rotation matrix lies in the following one dimensional subgroup of $\text{SO}(3)$:

$$R \in \left\{ R^\circ \exp [\theta S(b)] \mid \theta \in \mathbb{S}^1 \right\}. \quad (13)$$

B. Measurement error

We now consider the effects of small measurement errors. Let $\tilde{b} \in \mathbb{S}^2$ be the measured direction of the direction b . Since we only measure directions, we normalize b and \tilde{b} so that they have unit lengths. Therefore it is inappropriate to express the measurement error by a vector difference. The measurement error is modeled by rotation of the measured direction

$$\begin{aligned} b &= \exp [S(\nu)] \tilde{b}, \\ &\simeq \tilde{b} + S(\nu) \tilde{b}, \end{aligned} \quad (14)$$

where $\nu \in \mathbb{R}^3$ is the Euler axis of rotation from \tilde{b} to b , and $\|\nu\|$ is the corresponding rotation angle error in radians. The measurement error is bounded by an uncertainty ellipsoid

$$\nu \in \mathcal{E}_{\mathbb{R}^3}(0_3, S) \quad (15)$$

for a symmetric positive definite matrix $S \in \mathbb{R}^{3 \times 3}$. The magnitude of the measurement error is assumed to be small.

Let $\tilde{R}^\circ \in \text{SO}(3)$ be a rotation matrix obtained by (11) for the measured direction \tilde{b} . We express the difference between R° and \tilde{R}° using the exponential map:

$$R^\circ = \tilde{R}^\circ \exp [S(\zeta^\circ)] \quad (16)$$

for some $\zeta^\circ \in \mathbb{R}^3$. Since we make the small measurement error assumption, the norm of the vector ζ° is considered to be much smaller than π , i.e. $\|\zeta^\circ\| \ll \pi$. Since $e = R^\circ b = \tilde{R}^\circ \tilde{b}$, we obtain

$$\begin{aligned} \tilde{R}^\circ \tilde{b} &= R^\circ b, \\ &= \tilde{R}^\circ \exp [S(\zeta^\circ)] \{I_{3 \times 3} + S(\nu)\} \tilde{b}, \\ &\simeq \tilde{R}^\circ \{I_{3 \times 3} + S(\zeta^\circ + \nu)\} \tilde{b}, \end{aligned}$$

Thus we have $S(\zeta^\circ + \nu) \tilde{b} = 0$, which is equivalent to

$$\zeta^\circ = c\tilde{b} - \nu \quad (17)$$

for any constant $c \in \mathbb{R}$. Since $\|\zeta^\circ\| \leq |c| + \|\nu\| \ll \pi$, the constant c is smaller than π , i.e. $|c| \ll \pi$.

Substituting (14), (16), and (17) into (12), we obtain

$$R = \tilde{R}^\circ \exp [S(c\tilde{b} - \nu)] \exp [\theta S((I_{3 \times 3} + S(\nu))\tilde{b})] \quad (18)$$

for constants c and $\theta \in \mathbb{S}^1$.

In summary, if the single direction measurement has a small error represented by (14), then the attitude of the rigid body can be written in terms of the measured direction \tilde{b} and the measurement error ν as (18). This expression includes the uncertainty caused by the measurement error as well as the uncertainty due to the single direction measurement assumption. The constant $\theta^\circ \in \mathbb{S}^1$ to determine R° and \tilde{R}° is specified by the following estimation procedure.

IV. ATTITUDE ESTIMATION WITH A SINGLE DIRECTION MEASUREMENT

The deterministic estimation scheme using uncertainty ellipsoids is introduced first. A deterministic estimator for the attitude and the angular velocity of a rigid body is developed by using the preceding attitude determination scheme.

The subscript k denotes the k th discrete index. The superscript f denotes the variables related to the flow update, and the superscript m denotes the variables related to the measurement update. $\tilde{\cdot}$ denotes a measured variable, and $\hat{\cdot}$ denotes an estimated variable.

A. Deterministic estimation

We use deterministic bounded estimation using ellipsoidal sets, referred to as uncertainty ellipsoids, to describe the uncertainty and measurement noise. The estimation process has three steps similar to those in the Kalman filter: prediction, measurement, and filtering steps. We assume that the initial condition lies in a prescribed uncertainty ellipsoid, which is propagated in time using the equations of motion. This defines a prediction step. The measurement error bound is described by a measurement uncertainty ellipsoid. Then we can guarantee that the state lies in the intersection of the

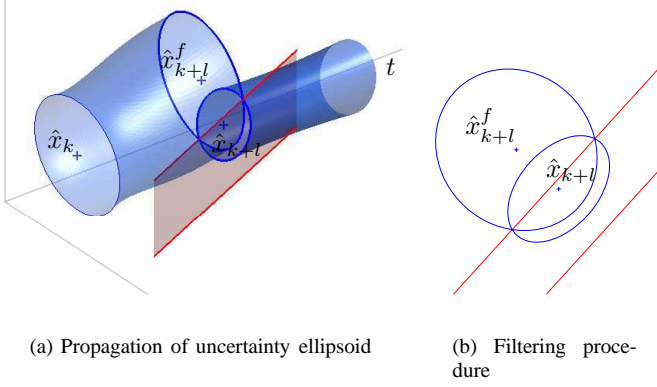


Fig. 1. Uncertainty ellipsoids

predicted uncertainty ellipsoid and the measured uncertainty ellipsoid. The intersection of the two ellipsoids is an irregular shape, which is not efficient to compute and store. Instead we find a minimal ellipsoid that contains this intersection. This procedure is repeated whenever new measurements are available.

This deterministic estimation procedure is illustrated in Fig. 1. The left figure shows time evolution of an uncertainty ellipsoid, and the right figure shows a cross section at a fixed measurement instant. At the k th time step, the state is bounded by an uncertainty ellipsoid centered at \hat{x}_k . This initial ellipsoid is propagated through time. Suppose that the state is measured next at the $(k + l)$ th time step. In this single direction measurement estimation, the measurement ellipsoid degenerates to a strip. At this instant, the actual state lies in the intersection. In the estimation process, we find a new ellipsoid that contains this intersection, as shown in the right figure. The center of the new ellipsoid, \hat{x}_{k+l} gives a point estimate of the state at time step $(k + l)$, and the magnitude of the new uncertainty ellipsoid measures the estimation accuracy. The deterministic estimates are optimal in the sense that the sizes of the ellipsoids are minimized.

B. Flow update

Suppose that the attitude and the angular momentum at the k th step lie in a given uncertainty ellipsoid:

$$(R_k, \Omega_k) \in \mathcal{E}(\hat{R}_k, \hat{\Omega}_k, P_k),$$

and a new measurement is taken at the $(k + l)$ th time step.

The flow update finds the center and the uncertainty matrix that define the uncertainty ellipsoid at the $(k + l)$ th step using the given uncertainty ellipsoid at the k th step. Since the attitude dynamics of a rigid body is nonlinear, the admissible boundary of the state at the $(k + l)$ th step is not an ellipsoid in general. We assume that the given uncertainty ellipsoid at the k th step is sufficiently small that attitudes and angular velocities in the uncertainty ellipsoids can be approximated using the linearized equations of motion. Then we can guarantee that the uncertainty set at the $(k + l)$ th step is an ellipsoid, and we can compute its center and its uncertainty matrix at the $(k + l)$ th step separately.

Center: For the given center at step k , $(\hat{R}_k, \hat{\Omega}_k)$, the center of the uncertainty ellipsoid at step $(k + l)$ is $(\hat{R}_{k+l}^f, \hat{\Omega}_{k+l}^f)$ obtained using the discrete equations of motion, (4), (5), and (6):

$$hS(J\hat{\Omega}_k + \frac{h}{2}\hat{M}_k) = \hat{F}_k J_d - J_d \hat{F}_k^T, \quad (19)$$

$$\hat{R}_{k+1}^f = \hat{R}_k \hat{F}_k, \quad (20)$$

$$J\hat{\Omega}_{k+1}^f = \hat{F}_k^T \hat{\Omega}_k + \frac{h}{2}\hat{F}_k^T \hat{M}_k + \frac{h}{2}\hat{M}_{k+1}. \quad (21)$$

This integrator yields a map $(\hat{R}_k, \hat{\Omega}_k) \mapsto (\hat{R}_{k+1}^f, \hat{\Omega}_{k+1}^f)$, and this process is repeatedly applied to find the center at the $(k + l)$ th step, $(\hat{R}_{k+l}^f, \hat{\Omega}_{k+l}^f)$.

Uncertainty matrix: We assume that an uncertainty ellipsoid contains small perturbations from the center of the uncertainty ellipsoid. Then the uncertainty matrix is propagated by using the linearized flow of the discrete equations of motion. At the $(k + 1)$ th step, the uncertainty ellipsoid is represented by perturbations from the center $(\hat{R}_{k+1}^f, \hat{\Omega}_{k+1}^f)$ as

$$R_{k+1} = \hat{R}_{k+1}^f \exp S(\zeta_{k+1}^f), \\ \Omega_{k+1} = \hat{\Omega}_{k+1}^f + \delta\Omega_{k+1}^f,$$

for some $\zeta_{k+1}^f, \delta\Omega_{k+1}^f \in \mathbb{R}^3$. The uncertainty matrix at the $(k + 1)$ th step is obtained by finding a bound on $\zeta_{k+1}^f, \delta\Omega_{k+1}^f \in \mathbb{R}^3$. Assume that the uncertainty ellipsoid at the k th step is sufficiently small. Then, $\zeta_{k+1}^f, \delta\Omega_{k+1}^f$ are represented by the following linear equations using the results presented in [13]

$$x_{k+1}^f = A_k^f x_k,$$

where $x_k = [\zeta_k; \delta\Omega_k] \in \mathbb{R}^6$, and $A_k^f \in \mathbb{R}^{6 \times 6}$ can be suitably defined. Since $(R_k, \Omega_k) \in \mathcal{E}(\hat{R}_k, \hat{\Omega}_k, P_k)$, $x_k \in \mathcal{E}_{\mathbb{R}^6}(0, P_k)$ by the definition of the uncertainty ellipsoid given in (8). This implies that $A_k^f x_k$ lies in the following uncertainty ellipsoid

$$A_k^f x_k \in \mathcal{E}_{\mathbb{R}^6}\left(0, A_k^f P_k (A_k^f)^T\right).$$

Thus, the uncertainty matrix at the $(k + 1)$ th step is given by

$$P_{k+1}^f = A_k^f P_k (A_k^f)^T. \quad (22)$$

The above equation is then applied repeatedly to find the uncertainty matrix at the $(k + l)$ th step.

In summary, the uncertainty ellipsoid at the $(k + l)$ th step is computed using (19), (20), (21), and (22) as:

$$(R_{k+l}, \Omega_{k+l}) \in \mathcal{E}(\hat{R}_{k+l}^f, \hat{\Omega}_{k+l}^f, P_{k+l}^f), \quad (23)$$

C. Measurement update

The measurement update finds an uncertainty ellipsoid in the state space using the measurement and the measurement error models described in Section III. A feasible set of rotation matrices that is compatible with the single direction measurement is described in (18). We find an expression for

the measurement uncertainty ellipsoid such that it contains the set described by (18).

Elements in the measurement uncertainty ellipsoid are expressed as

$$R_{k+1} = \hat{R}_{k+l}^m \exp S(\zeta_{k+l}^m) \quad (24)$$

for the center $\hat{R}_{k+l}^m \in \text{SO}(3)$ and some $\zeta_{k+l}^m \in \mathbb{R}^3$. We omit the subscript $(k+l)$ hereafter for convenience, and it is assumed that the direction is measured at the $(k+l)$ th step.

Center: Comparing (18) and (24), we choose the center of the measurement uncertainty ellipsoid as

$$\begin{aligned} \hat{R}^m &= \tilde{R}^\circ, \\ &= \exp \left[\cos^{-1}(\tilde{b}^T e) S \left(\frac{\tilde{b} \times e}{\|\tilde{b} \times e\|} \right) \right] \exp S(\theta^\circ \tilde{b}), \end{aligned} \quad (25)$$

for the constant $\theta^\circ \in S^1$ which is determined by the following filtering procedure.

Uncertainty Matrix: From (18) and (24), we have

$$\exp S(\zeta^m) \exp[-S(c\tilde{b} - \nu)] = \exp[\theta S((I_{3 \times 3} + S(\nu))\tilde{b})].$$

Since the vectors ζ^m and $\zeta^\circ = c\tilde{b} - \nu$ are assumed to be small, the above equation is approximated as

$$\zeta^m - (c\tilde{b} - \nu) = \theta \tilde{b} + \theta S(\nu)\tilde{b},$$

which can be rewritten as

$$\begin{aligned} \zeta^m - (\theta + c)\tilde{b} &= -\nu - \theta S(\tilde{b})\nu, \\ &= (\theta - 1)\nu - \theta(I_{3 \times 3} + S(\tilde{b}))\nu. \end{aligned}$$

Since $\nu \in \mathcal{E}_{\mathbb{R}^3}(0_3, S)$ and $\theta \in \mathbb{S}^1$, the terms in the right hand side satisfy

$$\begin{aligned} (\theta - 1)\nu &\in \mathcal{E}_{\mathbb{R}^3}(0_3, (1 + \pi)^2 S), \\ \theta(I_{3 \times 3} + S(\tilde{b}))\nu &\in \mathcal{E}_{\mathbb{R}^3}(0_3, \pi^2 \mathcal{A}^{m,T} S \mathcal{A}^m), \end{aligned}$$

where $\mathcal{A}^m = I_{3 \times 3} + S(\tilde{b}) \in \mathbb{R}^{3 \times 3}$. Therefore, the vector $\zeta^m - (\theta + c)\tilde{b}$ lies in an ellipsoid containing the vector sum of the above two ellipsoids. The expressions for the minimal ellipsoid containing the vector sum of two ellipsoids are given in [11]. Using the results, we have

$$\zeta^m - (\theta + c)\tilde{b} \in \mathcal{E}_{\mathbb{R}^3}(0_3, P_0^m), \quad (26)$$

where

$$\begin{aligned} P_0^m &= (1 + q^{-1})Q^1 + (1 + q)Q^2, \quad q = \sqrt{\frac{\text{tr}[Q^1]}{\text{tr}[Q^2]}}, \\ Q^1 &= (1 + \pi)^2 S, \quad Q^2 = \pi^2 \mathcal{A}^{m,T} S \mathcal{A}^m. \end{aligned}$$

From (26), we can guarantee that the vector ζ^m lies in an ellipsoid containing the following union of the sets

$$\mathcal{E}_{\mathbb{R}^3}(-\pi\tilde{b}, P_0^m) \cup \mathcal{E}_{\mathbb{R}^3}(\pi\tilde{b}, P_0^m).$$

This is a consequence of the fact that an ellipsoid is convex and the assumption $|c| \ll \pi$. The ellipsoid that contains the

union of two ellipsoids is obtained numerically by the LMI approach presented in [15].

$$\mathcal{E}_{\mathbb{R}^3}(0_3, P^m) \supset \left(\mathcal{E}_{\mathbb{R}^3}(-\pi\tilde{b}, P_0^m) \cup \mathcal{E}_{\mathbb{R}^3}(\pi\tilde{b}, P_0^m) \right). \quad (27)$$

In summary, a single direction measurement with small error guarantees that the rotation matrix is expressed as (24), where the center \hat{R}^m is given by (25), and the vector ζ^m lies in the uncertainty ellipsoid given by (27).

D. Filtering procedure

The filtering procedure finds a new uncertainty ellipsoid compatible with both the predicted uncertainty ellipsoid and the measured uncertainty ellipsoid. The intersection of two ellipsoids is generally not an ellipsoid. We find a minimal uncertainty ellipsoid containing the intersection.

The predicted uncertainty ellipsoid is based on \hat{R}^f and the measurement ellipsoid is based on \hat{R}^m . In the following development, we assume that the difference between the rotation matrices \hat{R}^f and \hat{R}^m is small. Here we find a value of $\theta^\circ \in \mathbb{S}^1$ at (25) such that the difference is minimized. Define an index $\mathcal{J} = \text{tr}[I_{3 \times 3} - \hat{R}^{f,T} \hat{R}^m]$. A standard variational approach with the use of Rodriguez formula shows that the index is minimized when

$$\theta^\circ = -\tan^{-1} \frac{\text{tr}[\hat{R}^{f,T} \tilde{R}^\Delta S(\tilde{b})]}{\text{tr}[\hat{R}^{f,T} \tilde{R}^\Delta S(\tilde{b})^2]},$$

$$\text{tr}[\hat{R}^{f,T} \tilde{R}^\Delta S(\tilde{b})] \sin \theta^\circ - \text{tr}[\hat{R}^{f,T} \tilde{R}^\Delta S(\tilde{b})^2] \cos \theta^\circ > 0,$$

where $\tilde{R}^\Delta \in \text{SO}(3)$ is the first exponential of (25). The first equation is obtained by the optimality condition $\frac{\partial \mathcal{J}}{\partial \theta^\circ} = 0$, and the second inequality is obtained by $\frac{\partial^2 \mathcal{J}}{\partial (\theta^\circ)^2} > 0$. These conditions define the value of $\theta^\circ \in \mathbb{S}^1$ uniquely.

We find a minimal ellipsoid containing the intersection of the predicted uncertainty ellipsoid and the measurement uncertainty ellipsoid. An element in the predicted uncertainty ellipsoid, $(R^f, \Omega^f) \in \mathcal{E}(\hat{R}^f, \hat{\Omega}^f, P^f)$, can be written as

$$R^f = \hat{R}^f e^{S(\zeta^f)}, \quad (28)$$

$$\Omega^f = \hat{\Omega}^f + \delta\Omega^f, \quad (29)$$

for some $(\zeta^f, \delta\Omega^f) \in \mathcal{E}_{\mathbb{R}^6}(0_{6 \times 1}, P^f)$. We find an equivalent expression based on the measurement ellipsoid center \hat{R}^m . Define $\hat{\zeta}^{mf} \in \mathbb{R}^3$ such that

$$\hat{R}^f = \hat{R}^m e^{S(\hat{\zeta}^{mf})}. \quad (30)$$

Thus, $\hat{\zeta}^{mf}$ represents the difference between the centers of the two ellipsoids. Substituting (30) into (28),

$$\begin{aligned} R^f &= \hat{R}^m e^{S(\hat{\zeta}^{mf})} e^{S(\zeta^f)}, \\ &\simeq \hat{R}^m e^{S(\hat{\zeta}^{mf} + \zeta^f)}, \end{aligned}$$

where we assumed that $\hat{\zeta}^{mf}, \zeta^f$ are sufficiently small to obtain the second equality. Thus, the uncertainty ellipsoid obtained by the flow update, $\mathcal{E}(\hat{R}^f, \hat{\Omega}^f, P^f)$ is identified by the center $(\hat{R}^m, \hat{\Omega}^f)$ and the uncertainty ellipsoid in \mathbb{R}^6 .

$$(\hat{\zeta}^{mf}, \delta\Omega^f) \in \mathcal{E}_{\mathbb{R}^6}(\hat{x}^{mf}, P^f),$$

where $\hat{x}^{mf} = [\hat{\zeta}^{mf}; 0_3]$, and $S(\zeta^{mf}) = \logm(\hat{R}^{m,T}R^f) \in \mathfrak{so}(3)$, $\delta\Omega^f = \Omega^f - \hat{\Omega}^f \in \mathbb{R}^3$.

We seek a minimal ellipsoid that contains the intersection of the following uncertainty ellipsoids.

$$\left(\mathcal{E}_{\mathbb{R}^3}(0_3, P^m) \cap \mathcal{E}_{\mathbb{R}^6}(\hat{x}^{mf}, P^f)\right) \subset \mathcal{E}_{\mathbb{R}^6}(\hat{x}, P), \quad (31)$$

where $\hat{x} = [\hat{\zeta}^T, \delta\hat{\Omega}^T]^T \in \mathbb{R}^6$. Expressions for a minimal ellipsoid containing the intersection of two ellipsoids are presented in [11]. Using those results, \hat{x} and P are given by

$$\begin{aligned} \hat{x} &= (I_{6 \times 6} - LH)\hat{x}^{mf}, \\ P &= \beta(r)[(I - LH)P^f(I - LH)^T + r^{-1}LP^mL^T], \end{aligned}$$

where $L \in \mathbb{R}^{6 \times 3}$, $H \in \mathbb{R}^{3 \times 6}$, and $\beta(r) \in \mathbb{R}$ are given by

$$\begin{aligned} L &= P^f H^T [HP^f H^T + r^{-1}P^m]^{-1}, \\ H &= [I_{3 \times 3}, 0_{3 \times 3}]^T, \\ \beta(r) &= 1 + r - (\hat{x}^{mf})^T H^T [HP^f H^T + r^{-1}P^m]^{-1} H \hat{x}^{mf}, \end{aligned}$$

for a constant r , which is chosen such that $\text{tr}[P]$ is minimized.

In summary, a new uncertainty ellipsoid at the $(k+l)$ th step is given by

$$(\mathcal{R}_{k+1}, \Omega_{k+1}) \in \mathcal{E}(\hat{R}_{k+1}, \hat{\Omega}_{k+1}, P_{k+1}), \quad (32)$$

where

$$\hat{R}_{k+1} = \hat{R}_{k+1}^m e^{S(\hat{\zeta})}, \quad (33)$$

$$\hat{\Omega}_{k+1} = \hat{\Omega}_{k+1}^f + \delta\hat{\Omega}, \quad (34)$$

$$P_{k+1} = P. \quad (35)$$

The entire procedure is repeated whenever a new measurement is available.

The steps outlined above define a dynamic filter. The center of the uncertainty ellipsoid is considered as a point estimate of the attitude and the angular velocity at the $(k+l)$ th step. The uncertainty matrix represents the characteristics of the uncertainty, and the size of the uncertainty matrix represents the accuracy of the estimate. If the size of the uncertainty ellipsoid is small, we conclude that the estimate is accurate. This estimation is optimal in the sense that the size of the filtered uncertainty ellipsoid is minimized.

E. Properties of the estimator

The notable feature of this attitude estimator is that it requires a single direction measurement. Current attitude estimators based on the solution of Wahba's problem require at least two direction measurements at each instant. A single direction measurement provides only a two-dimensional constraint for the six-dimensional tangent bundle. The information obtained from the attitude dynamics is utilized, together with the measurement, in order to estimate the attitude and the angular velocity of the rigid body. In this paper, it is assumed that the angular velocity is not measured, but the current results can be readily extended to incorporate angular velocity measurements.

This attitude estimator has no singularities since the attitude is represented by a rotation matrix, and the geometric structure of the rotation matrix is preserved since it is updated by the structure-preserving Lie group variational integrator. The presented estimator can be used for highly nonlinear large angle maneuvers of a rigid body. It is also robust to the distribution of the measurement noise since we only use ellipsoidal bounds on the noise. The measurements need not be periodic, the estimation is repeated whenever new measurements become available.

V. NUMERICAL EXAMPLE

Numerical simulation results are given for the estimation of the attitude dynamics of an uncontrolled rigid spacecraft in a circular orbit about a large central body, including gravity gradient effects. The details of the on orbit spacecraft model are presented in [13].

The mass, length and time dimensions are normalized by the mass of the spacecraft, the maximum length of the spacecraft, and the orbital angular velocity, respectively. The moment of inertia of the spacecraft is chosen as $J = \text{diag}[1, 2.8, 2]$. The maneuver is a large attitude change completed in a quarter of the orbit. The initial conditions are chosen as

$$\begin{aligned} R_0 &= \begin{bmatrix} 0.707 & -0.707 & 0 \\ 0.707 & 0.707 & 0 \\ 0 & 0 & 1 \end{bmatrix}, & \Omega_0 &= [2.32, 0.45, -0.59], \\ \hat{R}_0 &= I_{3 \times 3}, & \hat{\Omega}_0 &= [2.12, 0.55, -0.89]. \end{aligned}$$

The corresponding initial estimation errors are $\|\zeta_0\| = 45 \text{ deg}$, $\|\delta\Omega_0\| = 21.43 \frac{\pi}{180} \text{ rad/s}$. Note that the actual initial attitude is opposite to the estimated initial attitude. The initial uncertainty matrix is given by

$$P_0 = \text{diag}[2.28, 2.28, 2.28, 0.82, 0.82, 0.82],$$

so that $x_0^T P_0^{-1} x_0 = 0.857 \leq 1$.

We assume that the measurements are available twenty times. The inertial direction e to a known point is chosen from the columns of the following matrix.

$$E = \begin{bmatrix} 1 & 0 & 0 & 0.7071 & -0.7071 & 0.5 & -0.5 \\ 0 & 1 & 0 & 0.7071 & 0.7071 & 0.5 & 0.5 \\ 0 & 0 & 1 & 0 & 0 & 0.7071 & 0.7071 \end{bmatrix}.$$

A simple adaptive scheme is developed to choose the best inertial direction as the spacecraft rotates. The uncertainty matrix for the measurement noise is given by

$$S_k = \left(0.2 \frac{\pi}{180}\right)^2.$$

The direction measurement noise is normally distributed in the simulation.

Fig. 2 shows simulation results, where the left figure shows the attitude estimation error and the angular velocity estimation error, and the right figure shows the size of the uncertainty ellipsoid. The estimation errors and the size of the uncertainty are reduced rapidly after the first few measurements; the estimation error for the angular velocity

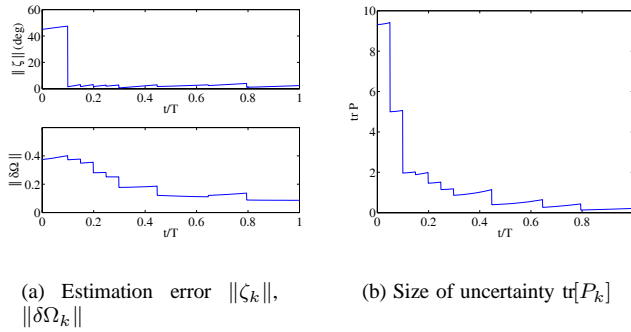


Fig. 2. Estimation errors and uncertainty

converges relatively slowly since the angular velocity is not measured directly. The terminal attitude error, and the terminal angular velocity error are less than 2.3 deg, and 0.08 rad/s, respectively.

VI. CONCLUSIONS

A deterministic attitude estimator for a rigid body under an attitude dependent potential is developed. This estimator requires only a single direction measurement to a known reference point at each measurement instant. A feasible set of rotation matrices compatible with the measurement is described in terms of Lie algebra elements, and it is compared with an uncertainty ellipsoid obtained from an attitude dynamics model, in order to obtain an updated attitude estimate. The attitude is globally represented by a rotation matrix, and the geometric structure of the rotation matrix is preserved by using a Lie group variational integrator.

REFERENCES

- [1] G. Wahba, "A least squares estimate of satellite attitude, Problem 65-1," *SIAM Review*, vol. 7, no. 5, p. 409, 1965.
- [2] J. L. Farrell, J. C. Stuelpnagel, R. H. Wessner, J. R. Velman, and J. E. Brock, "A least squares estimate of satellite attitude, Solution 65-1," *SIAM Review*, vol. 8, no. 3, pp. 384–386, 1966.
- [3] M. D. Shuster and S. D. Oh, "Three-axis attitude determination from vector observations," *Journal of Guidance Control and Dynamics*, vol. 4, no. 1, pp. 70–77, 1981.
- [4] A. K. Sanyal, "Optimal attitude estimation and filtering without using local coordinates, Part I: Uncontrolled and deterministic attitude dynamics," in *Proceedings of the American Control Conference*, 2006, pp. 5734–5739.
- [5] M. D. Shuster, "Kalman filtering of spacecraft attitude and the QUEST model," *Journal of the Astronautical Sciences*, vol. 38, no. 3, pp. 377–393, 1990.
- [6] M. L. Psiaki, "Attitude determination filtering via extended quaternion estimation," *AIAA Journal of Guidance, Control and Dynamics*, vol. 23, no. 2, pp. 206–214, 2000.
- [7] T. Lee, A. Sanyal, M. Leok, and N. H. McClamroch, "Deterministic global attitude estimation," in *Proceedings of the IEEE Conference on Decision and Control*, 2006.
- [8] M. D. Shuster, "Deterministic three-axis attitude determination," *The Journal of the Astronautical Sciences*, vol. 52, no. 3, pp. 405–419, 2004.
- [9] Y. Theodor, U. Shaked, and C. E. de Souza, "A game theory approach to robust discrete-time H_∞ -estimation," *IEEE Transactions on Signal Processing*, vol. 42, no. 6, pp. 1486–1495, 1994.
- [10] F. C. Schweppe, "Recursive state estimation: Unknown but bounded errors and system inputs," *IEEE Transactions on Automatic Control*, vol. 13, no. 1, pp. 22–28, 1968.

- [11] D. G. Maksarov and J. P. Norton, "State bounding with ellipsoidal set description of the uncertainty," *International Journal of Control*, vol. 65, no. 5, pp. 847–866, 1996.
- [12] C. Durieu, E. Walter, and B. Polyak, "Multi-input multi-output ellipsoidal state bounding," *Journal of Optimization Theory and Applications*, vol. 111, no. 2, pp. 273–303, 2001.
- [13] T. Lee, M. Leok, and N. H. McClamroch, "Attitude maneuvers of a rigid spacecraft in a circular orbit," in *Proceedings of the American Control Conference*, 2006, pp. 1742–1747.
- [14] —, "A Lie group variational integrator for the attitude dynamics of a rigid body with applications to the 3D pendulum," in *Proceedings of the IEEE Conference on Control Applications*, 2005, pp. 962–967.
- [15] S. Body, L. E. Ghaoui, E. Feron, and V. Balakrishnan, *Linear Matrix Inequalities in System and Control Theory*. SIAM, 1994.